VI International Conference on Computational Methods in Marine Engineering
MARINE 2015
F. Salvatore, R. Broglia and R. Muscari (Eds)

RANS-BASED OPTIMIZATION OF THE AFT PART OF SHIPS INCLUDING FREE SURFACE EFFECTS

A. VAN DER PLOEG

Maritime Research Institute Netherlands (MARIN)
6700 AA Wageningen
a.v.d.ploeg@marin.nl

Key words: Computational Fluid Dynamics, Optimisation, Scale Effects.

Abstract. A procedure for optimizing the aft body of a ship for minimal power and best wake field quality is described, based on full-scale RANS computations possibly including free-surface effects. A flexible and effective definition of parametric hull form variations is used, based on interpolation between a limited number of basis hull forms. This keeps the dimension of the search space low, which enables to do systematic variations. For a test case in which the ship's wave making can be neglected it is shown that the grid dependence in the computed trends is low, and for a test case including free-surface effects it is demonstrated how the search space can be set up in such a way that a considerable decrease in required power can be obtained without spoiling the wake quality.

1 INTRODUCTION

Optimization procedures based on CFD-computations are becoming increasingly important in practical ship design projects. Potential-flow solvers are used routinely nowadays to optimize the front part of ships, for example, in order to minimize wave resistance. For the aft part of ships however, viscous effects can have a significant influence and need therefore be modeled correctly. The optimization has to be done at full scale, since scale effects, for example, in the wake fields, the stern wave pattern or the amount of flow separation can significantly influence the trends in the propulsive parameters ([10] and [13]). An example of such a scale effect for a flow near a transom is shown in Figure 1. This figure shows the wave elevation aft of the transom with the predicted axial velocity in main stream direction projected on the free surface as colored contours. Black colors indicate regions with flow reversal. It appears that the transom flow regime completely changes from model to full scale. More of such scale effects, as well as comparisons with available measurements are discussed in [10].

In this paper, we describe how Reynolds-Averaged Navier-Stokes (RANS) solvers can be used for optimization of the aft part of ships. A very large numerical accuracy of the evaluation of the objective functions is required, as otherwise the predicted trends are polluted or spoilt by numerical errors. Therefore, the grids need to be fine enough to guarantee that grid dependence does not influence the computational trends and the acceptance criterion needs to be set sufficiently strict such that the effect of iterative errors becomes negligible. As a result, most RANS codes require large computation times, which make optimization, with

hundreds or thousands of calculations, impractically time-consuming. Alternative approaches are proposed in the literature using surrogate models, response surfaces etc. This can be successful but requires additional research and experience ([14]).

In this paper, we describe a different approach in which the dimension of the search space is kept low which allows us to do systematic variations. Of course, this requires a flexible and effective definition of parametric hull form variations, as well as an efficient viscous flow solver. These are described in Section 3. Section 2 first describes the choice of the object functions. Section 4 shows a grid dependence study for the computed Pareto fronts for a case in which free surface effects can be neglected, Section 5 describes how to include the ship's wave making and Section 6 gives an application of an optimization of the ship's aft body including free surface effects.

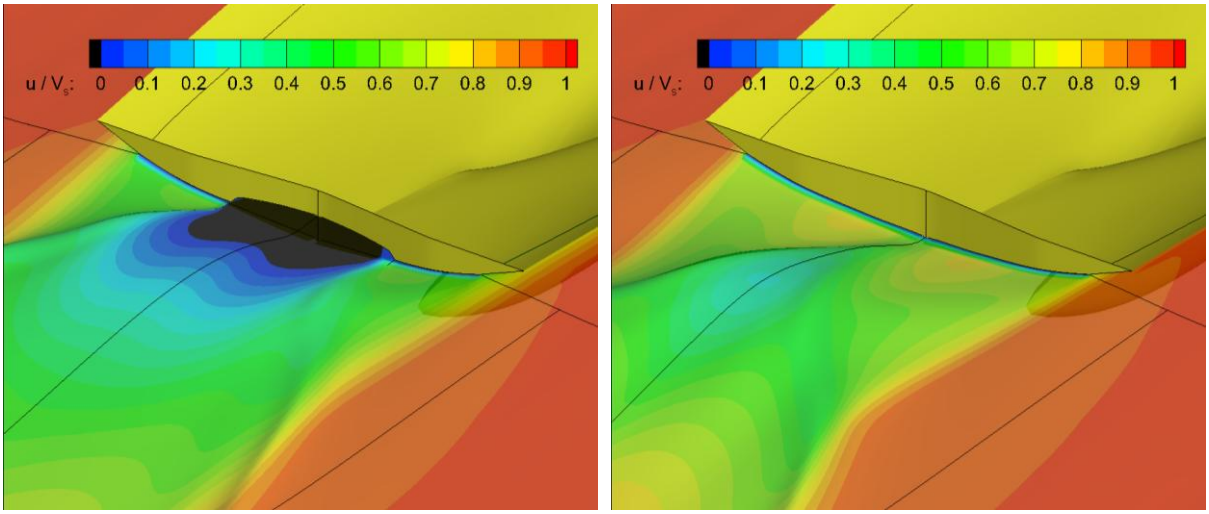

Figure 1 Example of a computed scale effect on the flow off a transom. Partly wetted at model scale (left), dry at full scale (right).

2 OBJECT FUNCTIONS

The choice of object functions is of crucial importance in hull form optimization projects. We will optimize the hull form for two object functions simultaneously, the first being an estimate of the required power to sustain a given speed, and the second a function that expresses the wake quality.

2.2 Power estimate

A decrease of the resistance is often accompanied by a relatively strong decrease of the nominal wake fraction. It is important to take this effect into account. Therefore, in this paper we evaluate as first object function not the resistance but an estimate of the power delivered to the propulsor:

$$P_D = \frac{R_T \times (1-w)}{1-t} \times \frac{V_S}{\eta_R \times \eta_0} \tag{1}$$

in which R_T is the towing resistance, w the estimated effective wake fraction, V_s the ship's speed, t the thrust deduction coefficient, η_o the propeller efficiency in open water, and η_R the relative rotative efficiency. The latter is approximated by 1, while η_o is obtained from the B-series of propellers ([4]). For each hull form, the computed nominal resistance R_T, and the hull efficiency $\eta_H=(1-t)/(1-w)$ is required to perform this evaluation. To compute the thrust deduction t, we also perform a second RANS computation including a force distribution representing the propeller with an imposed thrust T_0 which is in the neighbourhood of the thrust T required for self propulsion, such that we can assume a linear behavior of the force on the hull as a function of the imposed thrust. The thrust deduction coefficient can then be computed from $t=(R_0-R_T)/T_0$, in which R_0 is the resistance force resulting from the second RANS computation.

2.3 Wake object function

Scale effects in the wake field can be quite significant. Therefore, we propose a wake object function for the full-scale wake. In case of danger of erosive cavitation, one would like to prevent strong variations of the wake in circumferential direction, especially in the top half of the propeller plane. We will use the L1-norm of the variation of the undisturbed propeller inflow angle

$$\beta = \tan^{-1}\left(V_x / \left(\omega \tfrac{r}{R} - V_\theta\right)\right)$$

with V_x and V_θ the axial and tangential velocity components respectively, θ the angular position in rad. and ω the propeller rotation rate in rad/s. The variation of β in circumferential direction as the propeller rotates is $\partial\beta/\partial\theta$. The L1-norm is determined from integration in circumferential direction and over a range of radii from the hub to the tip and the propeller radius:

$$WOF \equiv \frac{\int_{r=hub}^{r=tip} \oint_\theta \left|\frac{\partial\beta}{\partial\theta}\right| f(\theta,r)\, d\theta dr}{\int_{r=hub}^{r=tip} \oint_\theta f(\theta,r)\, d\theta dr} \tag{2}$$

Herein f is a weighting function that can be used to make the outer region and/or the top region of the propeller more important.

3 EVALUATION OF THE OBJECT FUNCTIONS

A flexible and effective definition of parametric hull form variations is used, based on interpolation between a limited number of basis hull forms that span the design space. As a first step, some basis hull forms are created by whatever means (e.g. manually). Any design experience can be used in the choice of the basis hull forms, or specific and effective variations can be selected based on a first CFD computation for the original hull. Next, the in-house tool GMS-Merge [2] interpolates between these variations. In this way, a search space

is defined which has relatively few dimensions. The Condor system is used to run many computations in parallel on a cluster of available PCs. This allows doing systematic variations: for each hull form generated by GMS-merge, the object functions are evaluated.

As described in the previous section, the evaluation of the first object function requires two full-scale RANS computations.

3.1 RANS solver

We use the viscous flow solver PARNASSOS [1], which has a solution technique that is very efficient with respect to both CPU-time and memory usage [7], which makes it very well suited for doing systematic variations or combination with an optimization strategy [9]. It computes the steady, turbulent flow around ship hulls by solving the discretised Reynolds-averaged Navier-Stokes equations for steady, incompressible flow. It is a finite-difference method and around the ship structured, HO-type body-fitted grids are used with a very strong contraction in wall-normal direction towards the hull in order to have y^+-values below 1 near the wall, even for full-scale computations.

3.2 Computational domain

The inflow boundary is located $0.5L_{pp}$ in front of the bow, and the outflow boundary at $1.5L_{pp}$ behind the transom. Due to symmetry considerations, only the starboard side is taken into account. In an (x,y,z)-co-ordinate system fixed to the ship, with x positive aft and z upward, the lateral outer boundary is a quarter of a cylinder with axis $y=z=0$ and radius $1.0L_{pp}$. At this boundary tangential velocities and pressure found from a potential-flow computation are imposed. Since that computation gives good results already for much of the wave pattern, these boundary conditions (although of Dirichlet type for the pressure) hardly cause any wave reflection.

3.2 Automatic grid generation

Grids need to be generated around each variant and a fully automatic grid generation procedure is therefore required. To minimize the effect of discretization errors on the computed trends, these grids have to be as similar as possible. As a first step in the construction of the grid for a hull form variant, the wall grid for the original hull form is projected on the variant. Next, the 3D-grid is obtained using the usual grid-generation techniques: for this we use in-house developed elliptic grid generation software, which solves a Poisson equation to have maximal orthogonality of the gridlines in the interior of the computational domain. Near the boundaries, orthogonality can be controlled by the user. These settings are chosen the same for all hull forms.

4 EXAMPLE OF A GRID DEPENDENCE STUDY

In the European project VIRTUE, an EC-funded project under the 6th Framework program, procedures for multi-objective optimization of ship hulls were developed by various participants. This culminated in a workshop in which these procedures were applied to a common initial hull form design, the so-called VIRTUE tanker. The Reynolds numbers at model and full scale were, respectively, 6.5e7 and 2.25e9. The optimization was performed

for model scale and the object functions were (1) and (2). In this case, the two-equation k-ω SST model by Menter [5] was used.
The black lines in the right picture in Figure 2 show the body plan of the original vessel, together with the blue line which indicates the geometric constraints which had to be met in order to leave sufficient room for the engine. Propeller location and main dimensions were fixed and the displacement was not allowed to decrease. Free surface effects were not taken into account: all computations were performed for double body flow. For the current test case, with Froude number 0.15, the assumption is that changes in the wave resistance due to hull form variations are smaller than the variations in the towing resistance. This assumption was checked afterwards by computing the wave resistance for both the original and optimized vessel using a non-linear potential flow code. In this particular case, a hull form located on the Pareto front with a 3% decrease in the required power was chosen as optimized hull form. The body plan of this hull form is shown in red in the left picture. In [8] and [9] more details, comparisons with measurements, trends in the solutions and scale effects for this test case are given. In this paper we show only the result of a grid dependence study.
The right picture shows the computed Pareto fronts obtained on two grid densities. The axis show the relative increase in both object functions compared to the original hull form. The 'best' ships have the lowest value for both object functions; hence they are as close to the lower-left corner as possible. As can be seen from the figure, there is a set of hull forms that show the best compromise in decreasing both object functions. This set is called the Pareto front. The red squares indicate computations on a coarse grid (1.7M cells), and black squares indicate fine grid (3.4M cells) computations. The fine grids were obtained after refinement in all directions. Blue lines connect computations for the same hull form on different grid densities, so the length of these lines gives an indication of the grid dependence. There are several groups of almost parallel, blue lines with approximately the same length, which indicates that there is not much scatter in the results.

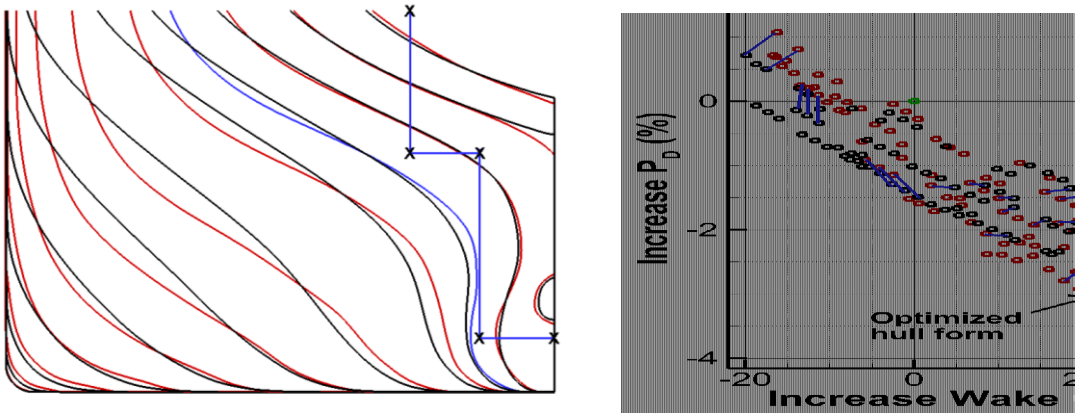

Figure 2 Left: Comparison of the body plans of the original VIRTUE tanker (black) and the optimized form (red). Right: Grid dependence study of the Pareto front for the using objective functions (1) and (2).

5 INCLUDING FREE-SURFACE EFFECTS

In practical ship design projects, one is often interested in the computation of the effect of stern wedges and stern flaps which can be used to improve the ship powering performance ([3]). In such applications, free-surface effects have to be taken into account. Especially, an accurate prediction of viscous free-surface flows near a ship's transom is important.
There exist many different methods to treat the interface between the water and the air above it. In [15] a review of three of those methods is given, by describing in detail their implementation in a particular code being used in industrial practice, together with examples of its use. A classification that is often used, is the division into two categories: surface fitting and surface capturing. In the latter the grid is held fixed and the free surface is modeled as an interface between two phases (air and water) somewhere in the middle of the computational domain, not matching any boundary of the grid. This has the advantage that there is in principle no limitation in the possible shape of the free surface (for example, breaking waves), but the drawback is that the interface will not be completely sharp. Therefore, in this paper we use a surface fitting approach: we compute single-phase flow (only water) and the upper boundary of the grid always matches the estimate of the free surface.
If we denote the velocity components by u,v,w, the wave height by $\zeta(x,y)$, and non-dimensionalise all quantities using the ship's speed U, a reference length L_{pp}, and gravity acceleration g, the free-surface boundary conditions are:

- a kinematic condition,
$$\zeta_t + u\zeta_x + v\zeta_y - w = 0 \quad \text{at} \quad z = \zeta \tag{3}$$
- a normal component of the dynamic condition, requiring that at the surface the pressure is atmospheric ($p=0$); neglecting surface tension and viscous contributions this takes the form
$$Fn^2\psi - \zeta = 0 \quad \text{at} \quad z = \zeta \tag{4}$$
in which $\psi=(p+\rho gz)/(\rho U^2)$ is the non-dimensional hydrodynamic pressure.
- Two tangential components of the dynamic condition, requiring that no shear stress is exerted on the water surface.

By substituting the wave elevation from the dynamic condition into the kinematic condition one obtains
$$Fn^2\left(u\psi_x + v\psi_y + w\psi_z\right) - w = 0 \quad \text{at} \quad z = \zeta \tag{5}$$
Together with the dynamic condition it describes exactly the same problem as the original set of conditions; but it has the advantage of permitting an iterative procedure solving directly the steady wave pattern without having to take into account any time dependent terms. We start with a grid of which the upper boundary matches a first estimate of the wavy surface, for example, estimated from a panel code, or simply an undisturbed water surface. Next, the following iterative method is used:

- Solve the RANS equations in which the combined condition (5) and the tangential dynamic conditions are imposed at the current estimate for the wave surface; this gives a new estimate for the wave surface.
- The new wave surface and grid are updated using the normal dynamic condition (4).

Each time after the RANS equations have been solved, corrections of trim and sinkage can be computed from the imbalance in forces and moments, and these corrections can be taken into account in the next grid update. Upon convergence the pressure deviation, normal velocity and shear stress vanish at the wave surface and the solution of the steady RANS/FS problem has been obtained.
In the present applications, the 'balanced discretization' as described in [12] has been used, which reduces the numerical damping of the waves to 5^{th} order in the longitudinal step size Δx, and the numerical dispersion to 3^{rd} order in the vertical spacing Δz. This contributes to a good accuracy of the wave pattern even at a distance from the hull.

5.2 Grid topology

As mentioned before, The RANS solver uses block-structured grids. To compute the flow off a transom, we use a special block topology that can handle both wetted and dry transoms, and even transoms that are partly dry and partly wetted. This topology consists of four blocks (Figure 3). The block upstream of the transom contains an HO-type body-fitted grid with the usual strong contraction in wall-normal direction towards the hull. It has a non-conformal matching with three blocks downstream of the transom, containing HH-type grids. The grid nodes in the block immediately behind the transom are contracted towards both the symmetry plane and the free surface to get sufficient resolution near the transom. The typical grid density we need of course depends on the wave length, and therefore on the Froude number. For the test case shown in Figure 3 the Froude number is 0.237 and the grid consists of 3.8 million cells for all four blocks together. In [10] it is shown for several hull forms that with this grid density the grid dependence in the computed flow and free surface is small, and that good agreement with available measurements can be obtained.

6 APPLICATION TO THE STREAMLINE TANKER

In the 7^{th}-Framework EU project "STREAMLINE" one work package was entirely devoted to the optimization of state-of-the-art propulsion. Part of the work consisted of the optimization of the aft part of the hull form and propeller of a chemical tanker that will be referred to as the 'STREAMLINE tanker'. The ship's speed is 14 knots, L_{pp}=*94m, B=15.4m*, the design draft is *6m* and the block coefficient is *0.786*. The Froude number is 0.237 and the full-scale Reynolds number is $6x10^8$. Again the displacement was not allowed to decrease and the propeller location as well as the ship's main dimensions was fixed. Constraints to guarantee sufficient room for machinery were that section 2 (the blue line shown in Figure 4) and all sections more upstream should stay outside a box indicated by the red lines.

As a first step, a RANS free-surface computation for the initial hull form was made. In this case, the one-equation model by Menter [6] was used. The grid is illustrated in Figure 3 and the grid density is discussed in the previous section.

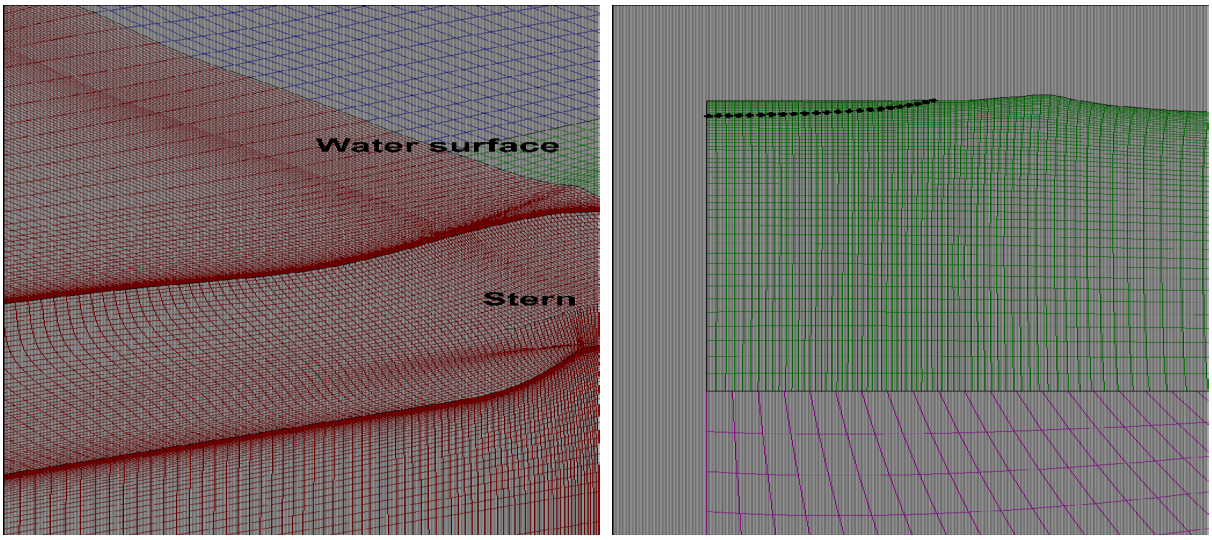

Figure 3 Left: bird's-eye view of the block topology. Right: a cross section of the computational mesh in the three blocks aft of the transom: the black dots indicates the transom edge in the upstream block.

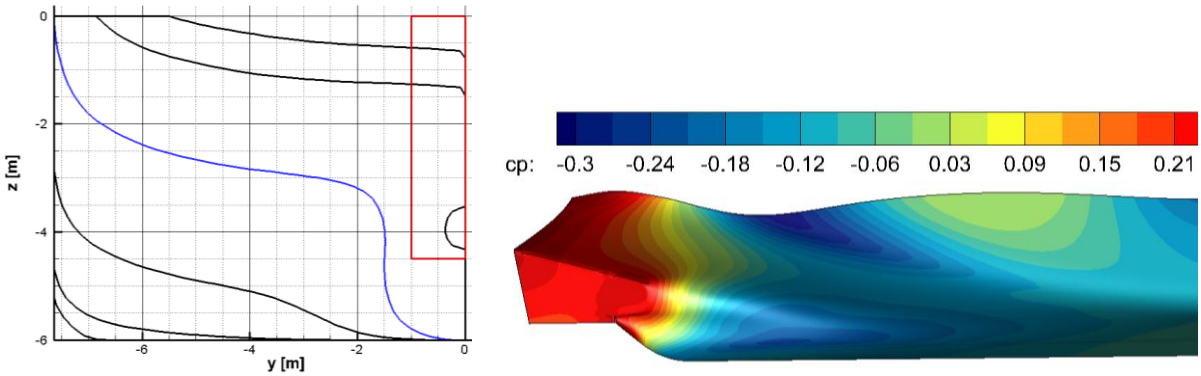

Figure 4 Left: body plan of the original STREAMLINE tanker, Red lines indicate required room for machinery. Right: dynamic pressure coefficient on this hull form.

The RANS/FS-study in [11] was restricted to the same design space used in combination with RANS/DB computations and the basis hull forms had relatively small changes compared to the original hull form near the water line. The right picture in Figure 4 shows the distribution of the pressure coefficient on the hull for the original vessel. It appears that there is an area with low pressure near the water line just in front of the propeller plane, which causes a relatively deep wave trough. Therefore, we enlarge the design space with new hull forms, allowing larger changes near the water line.

We have constructed two new basis hull forms that aim to reduce the wave resistance, by reducing the curvature in the geometry at this location. Those two extra basis hull forms are shown in Figure 5. The hull form shown on the right reduces the curvature in main stream direction; the one shown on the left reduces the curvature in girth wise direction.

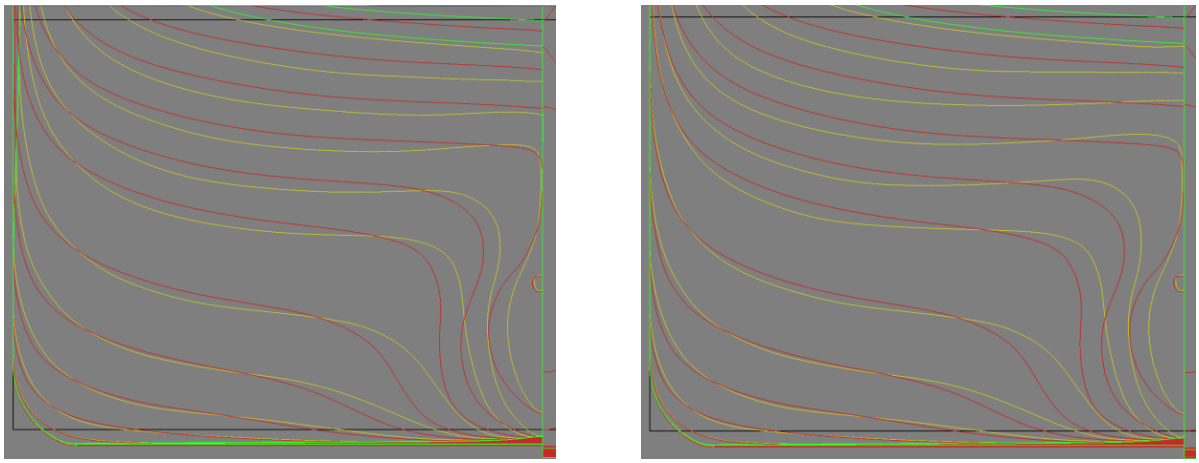

Figure 5 New basis hull forms with reduced curvature (yellow) compared to the original hull form (red).

In addition, a third basis hull form aims to increase the wetted part of the transom, and a fourth basis hull form has a more slender gondola. A systematic variation in the four-dimensional design space spanned by these hull forms was performed. From the computed Pareto fronts shown in Figure 6 it appears that a significant extra decrease in required power can be obtained in this design space. The first three candidate hull forms are discussed in [11]. The hull form Cand4 is the hull form on the Pareto front that shows the lowest required power and still a (slight) improvement of the wake quality.

This hull form is compared with the original hull form in Figure 6. It shows a combination of less curvature near the water line at the wave trough, a larger wetted part of the transom and a more slender gondola. The left picture in

Figure 7 shows that at the position near the waterline at the wave trough, indeed the pressure has increased, and the right picture shows that this results in a decrease of the wave trough. This figure also shows that closer to the transom, the reduced curvature along the waterline results in a significant decrease of the wave top. Although the recirculation zone aft of the transom has increased slightly (Figure 9), overall, the (nominal) resistance R_T has decreased with 4.5%. Together with a decrease of the product of efficiencies $\eta_0 \times \eta_H$ this results in a decrease of the estimate of the required power of 5.6%. A comparison of the wake fields is given in Figure 8.

7 CONCLUSIONS

The hull form variation technique described in Section 3 is defined by only a few, physically relevant, and ship-specific parameters. Hence the dimension of the search space is relatively low, which allows doing systematic variations of all parameters. We have described a procedure for evaluating an estimate for the required power and the wake quality at full scale. This requires two RANS computations for each hull form. The steady iterative approach described in Section 5 ensures that only a limited number of free surface updates are required, which helps to keep the required computational effort within reasonable bounds.

For the VIRTUE tanker it has been demonstrated that the grid dependence in the computed trends is limited. When free-surface effects were taken into account, a grid density was used for which in earlier work it was shown that the grid dependence is limited.

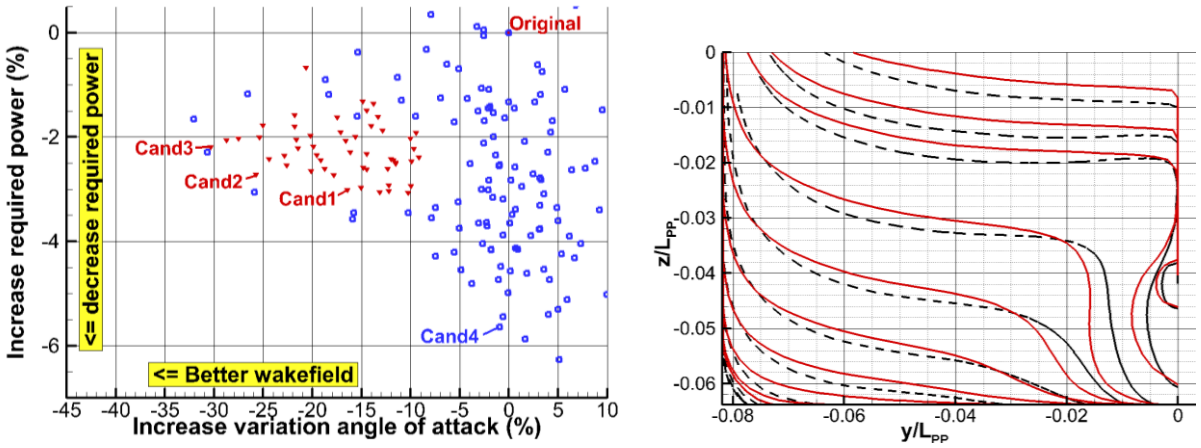

Figure 6 Left: Pareto fronts obtained with RANS/FS. Red triangles: same design space as used for RANS/DB. Blue squares: extended design space including hull forms with larger changes near the water line. Right: form Cand4 (black) compared with the original hull form (red).

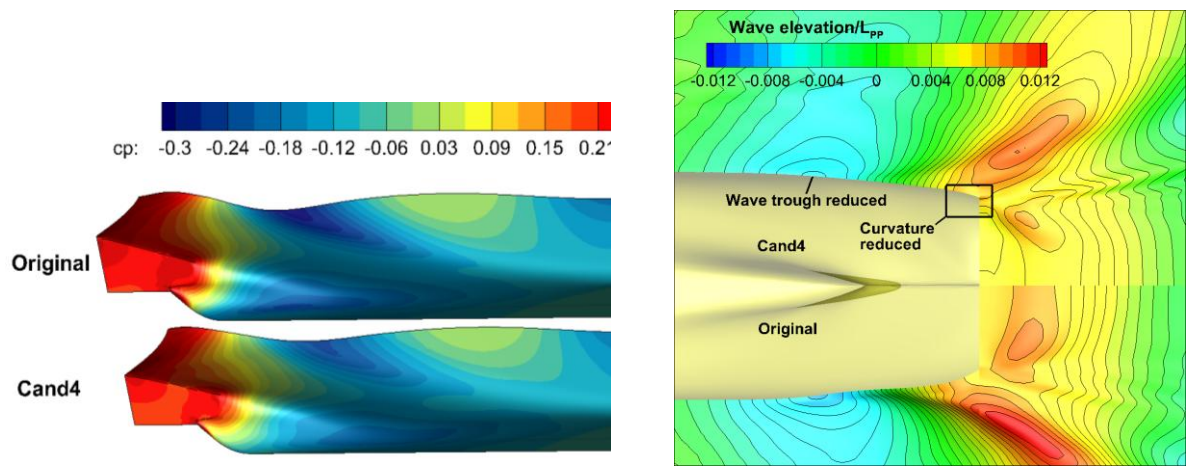

Figure 7 Left: comparison of the dynamic pressure coefficient on the hull. Right: Comparison of stern wave systems.

In a systematic variation of the aft body of the STREAMLINE tanker, in which the design space was enlarged with a number of hull forms based on an analysis of the pressure distribution, it appeared that a considerable decrease in required power (5.6%) can be obtained without decreasing the wake quality. We expect that using the experience from these systematic variations, other basis hull forms can be designed in such a way that a further improvement can be obtained.

The speed of PARNASSOS combined with parallelization over MARIN's PC network appeared to be very powerful. This combination allows doing a large number of RANS computations and to compute clear Pareto fronts. However, when free surface effects are included the required wall clock time using a cluster of modern PCs is about one weekend. For practical ship design projects it is desirable to reduce this to less than one night. Therefore, in the near

future we will study ways to accelerate the computation: a more efficient implementation of the RANS computations by exploiting graphical processors (GPU's) present in many of today's modern PCs, and reducing the required number of hull form evaluations by using response surfaces.

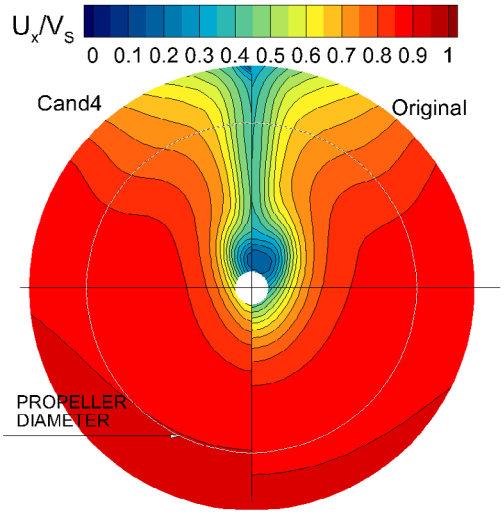

Figure 8 Comparison of nominal wake fields.

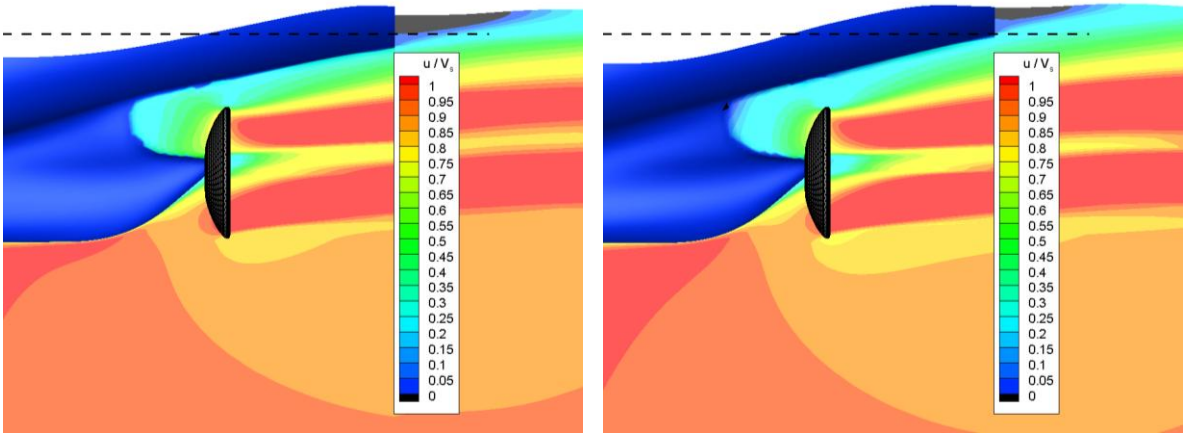

Figure 9 Comparison of the axial velocity in the centre plane near the propeller. Left: optimized hull. Right: original vessel.

REFERENCES

[1] Hoekstra M., (1999), *Numerical simulation of ship stern flows with a space-marching Navier Stokes method*, Thesis, Technical University of Delft.

[2] Hoekstra M. and Raven H.C., (2003), *A practical system for hydrodynamic optimisation of ship hull forms*, NAV 2003 Conference, Palermo, Italy.

[3] Karafiath G., Cusanelli D. and Cheng, W.L., (1999), *Stern Wedges and Stern Flaps for*

Improved Powering – U.S. Navy Experience. Sname Annual Meeting, Baltimore.
[4] Kuiper, G., (1992), *The Wageningen Propeller Series.* MARIN publication 92-001. Published on the occasion of its 60th anniversary.
[5] Menter, F.R., (1994) *Two-equation eddy-viscosity turbulence models for engineering applications*, AIAA Journal, Vol. 32, pp. 1598-1605.
[6] Menter, F.R. (1997), *Eddy viscosity transport equations and their relation to the k-ε model*, Jnl Fluid Eng. Vol. 119, pp. 876-884.
[7] Ploeg A. van der, Hoekstra M., and Eça L., (2000), *Combining accuracy and efficiency with robustness in ship stern flow computation,* Proc. 23rd Symp. Naval Hydrodynamics, Val de Reuil, France.
[8] Ploeg A. van der and Hoekstra M., (2009), *Multi-objective optimisation of a tanker after body using PARNASSOS*, Proceedings 12th NuTTs-symposium, Cortona.
[9] Ploeg A. van der and Raven H.C., (2010), *CFD-based Optimisation for Minimal Power and Wake Field Quality*, Proceedings 11th International Symposium on Practical Design of Ships and other Floating Structures, Rio de Janeiro, pp. 92-101.
[10] Ploeg A. van der and Starke A.R., (2011), *Prediction of the transom flow regime with viscous free surface computations,* International Conference on Computational Methods in Marine Engineering, Barcelona.
[11] Ploeg A. van der, Starke, A.R and Veldhuis, C., (2013), *Optimization of a chemical tanker with free-surface viscous flow computations*, Proceedings 12th International Symposium on Practical Design of Ships and other Floating Structures, Changwon City, Korea, pp. 716-723.
[12] Raven, H.C., Van der Ploeg, A. and Starke, A.R., (2004), *Computation of free-surface viscous flows at model and full scale by a steady iterative approach*, 25th Symposium on Naval Hydrodynamics, St. John's, Newfoundland, CANADA.
[13] Raven H.C., Ploeg A. van der, Starke A.R. Eça L., (2008), *Towards a CFD-based Prediction of Ship Performance ---Progress in Predicting Full-Scale Resistance and Scale Effects*, RINA MARINE CFD.
[14] Scholcz T.P., Gornicz T. and Veldhuis C., (2015), *Multi-objective hull-form optimization using Kriging on noisy computer experiments*. International Conference on Computational Methods in Marine Engineering, Rome.
[15] Wackers J., Koren B., Raven H.C., Ploeg A. van der, Starke A.R., Deng G.B., Queutey P., Visonneau M., Hino T. and Ohashi K., (2011), *Free-Surface Viscous Flow Solution Methods for Ship Hydrodynamics,* Arch Comput Methods Eng **18**: 1–41.